THE BELL SYSTEM TECHNICAL JOURNAL
Vol. 58, No. 10, December 1979
Printed in U.S.A.

A General Characterization of Splice Loss for Multimode Optical Fibers

By S. C. METTLER

(Manuscript received June 20, 1979)

The Gaussian point transmission model for calculating optical fiber splice loss is extended to the general case of splice loss between fibers which differ in one or more intrinsic parameters—core radius, index of refraction profile shape, and maximum index of refraction difference between core and cladding. The model is first verified for splices with index-of-refraction profile mismatch. The average difference between calculated and measured splice loss due to profile parameter mismatch is 0.04 dB. Comparisons are also made between calculated and measured splice loss for ten different splices with mismatch in all three intrinsic parameters. The average difference between the calculated loss and the average of several measured losses for these ten cases was 0.06 dB. The additional losses introduced by transverse offset measured for one set of mismatched fiber splices agree with the calculated values within 0.1 dB. Loss due to misalignment of elliptical core fibers is calculated and measured with agreement within 0.06 dB for the maximum loss case. Both the model and the experimental data show that, for a given percentage mismatch, index of refraction profile parameter mismatch and core ellipticity contribute significantly less to splice loss than mismatch of core radius or numerical aperture. A family of curves for splice loss vs transverse offset is presented for various numerical aperture mismatches and core radius mismatches, since these parameters are typically the largest components of splice loss in practical fiber optic systems.

I. INTRODUCTION

One factor which must be considered in the development of fiber optical communication systems is the effect of fiber core parameter manufacturing variations on splice loss. These intrinsic fiber core parameters[1] are the maximum index-of-refraction difference between

core and cladding, Δ, the index of refraction profile parameter, α, the radius, R, and core ellipticity, ϵ.

The development of a phenomenological Gaussian point loss model[2] allows an approximate analytic treatment of the loss induced by a butt-joint splice between fibers which differ in one or more intrinsic parameters. Previous models based on the uniform power distribution assumption[1] have exhibited only limited agreement between calculated and measured splice loss,[3,4] whereas the Gaussian model gives good agreement with experimental data.

Previous work[2] developed the Gaussian point loss model and gave theoretical and experimental results for Δ mismatch, R mismatch and transverse offset. This model has been used to estimate system losses due to random splicing between fibers whose intrinsic parameter variation distributions are known.[5] An extension of this model to the case of index-of-refraction profile (α) mismatch or ellipticity (ϵ), and to combinations of intrinsic factors plus transverse offset, is presented in this paper. Although the extension of the model is straightforward, the resulting calculations require the use of approximate numerical quadrature techniques applied over irregular areas of integration. This paper presents a unified analysis of the various effects of intrinsic factors and transverse offset on splice loss utilizing the Gaussian model. Representative experimental data are also presented.

II. THEORETICAL DEVELOPMENT

An approximate analytical treatment of the loss in a butt-joint splice between two fibers with differing intrinsic parameters can be carried out using a Gaussian model.[2] This model assumes that a steady-state power distribution (after a long length of fiber) can be modeled as a Gaussian distribution of the power within the solid angle defined by the local numerical aperture, NA, at any point on the fiber core (Fig. 1). With this assumed power distribution at the input to a splice, the ratio of the power received, p_2, at any radial position, r, to the power transmitted, p_1, at that point is related to the ratio of the squares of the NA's at that point by the following equation:[2]

$$t(r) = \frac{p_2}{p_1} = \begin{cases} 1 + \dfrac{(\mathrm{NA}_2)^2}{(\mathrm{NA}_1)^2} p_0 - e^{(\mathrm{NA}_2)^2/(\mathrm{NA}_1)^2 \ln p_0} & \text{for } \mathrm{NA}_2 < \mathrm{NA}_1 \\ 1 & \text{for } \mathrm{NA}_2 > \mathrm{NA}_1, \end{cases} \quad (1)$$

where p_0 is the point defining the width of the Gaussian distribution corresponding to 0.1 of its maximum. The expression $t(r)$ is called the point transmission function.

Using the usual class of circularly symmetric profiles,[1]

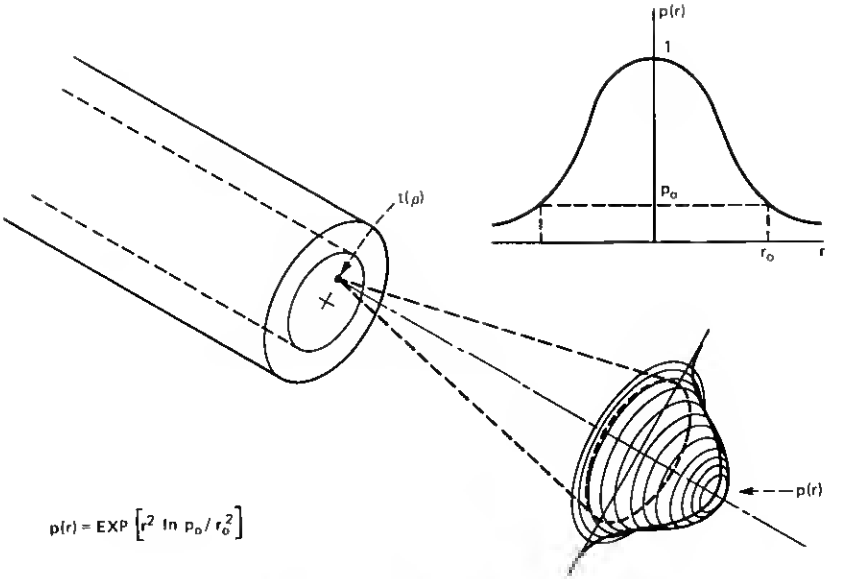

Fig. 1—Gaussian power distribution.

$$\mathrm{NA}(r) \simeq n_0 \sqrt{2\Delta} \left[1 - \left(\frac{r}{R}\right)^{\alpha}\right]^{1/2} \tag{2}$$

where $\Delta \simeq (n_0 - n_c)/n_0$ is small
n_0 = maximum core refractive index
n_c = refractive index of cladding
α = index profile parameter [$\alpha(r) = \alpha$]
R = fiber core radius.

Substituting eq. (2) into eq. (1) and defining

$$Q = \frac{(\mathrm{NA}_2)^2}{(\mathrm{NA}_1)^2} = \frac{\Delta_2(1 - r^{\alpha_2})}{\Delta_1(1 - k^{\alpha_1} r^{\alpha_1})} \tag{3}$$

gives the transmission coefficient at a radial distance r from the core axis,

$$t(r) = \begin{cases} 1 + Qp_0 - p_0^Q & \text{for } Q < 1 \\ 1. & \text{for } Q \geq 1, \end{cases} \tag{4}$$

where $k = R_2/R_1$ with R_2 normalized to 1. Subscripts 1 and 2 refer to the transmitting and receiving fibers respectively.

To find the total transmission through the splice, the point transmission function is multiplied by the input power of the transmitting fiber at each point and integrated over the area of core overlap. A

transmission ratio is obtained by dividing by the total input power:

$$T = \frac{P_2}{P_1} = \frac{\int_0^{2\pi} \int_0^{x} t(r)(1 - k^{\alpha_1} r^{\alpha_1})^2 r dr d\theta}{\int_0^{2\pi} \int_0^{1/k} (1 - k^{\alpha_1} r^{\alpha_1})^2 r dr d\theta}, \tag{5}$$

where x = the lesser of 1 or $1/k$.

For circularly symmetric profiles with no transverse offset:

$$T = \frac{P_2}{P_1} = \frac{\int_0^{x} t(r)(1 - k^{\alpha_1} r^{\alpha_1})^2 r dr}{\alpha_1^2 / 2k^2(\alpha_1 + 1)(\alpha_1 + 2)}. \tag{6}$$

This formula represents the total intrinsic loss immediately after the splice. Substitution of eq. (4) for $t(r)$ into (6) results in an integral which must be solved numerically for $t(r) \neq 1$ except for the special case of $\alpha_1 = \alpha_2$ and $R_1 = R_2$.

The inclusion of transverse offset in the problem requires the evaluation of the double integral in the numerator of eq. (5) over the area of overlap of the two fiber cores as shown in Fig. 2:

$$\frac{P_2}{P_1} = \frac{\int\int t(r)(1 - k^{\alpha_1} r^{\alpha_1})^2 r dr d\theta}{2\pi\alpha_1^2 / 2k^2(\alpha_1 + 1)(\alpha_1 + 2)}. \tag{7}$$

Equation (7), when integrated over the area of core overlap, represents a general solution for any combination of intrinsic mismatch and transverse offset for short receiving fibers. Long receiving fibers require the use of the long length $t(r)$ as given in Ref. 2. The splice loss can be calculated by evaluating Q at each point and integrating eq. (7) numerically using the appropriate expression for $t(r)$. This numerical integration can sometimes be simplified by careful consideration of the particular splice parameters. The absence of transverse offset, for example, reduces the numerator to a single integral in r for circularly symmetric fibers. These results assume flat, clean, perpendicular fiber ends with index-of-refraction matching fluid and no angular or longitudinal offset. In addition, a steady-state distribution is assumed at the input to the splice, requiring either a long input fiber or a launched power distribution approximating the steady state.

III. COMPARISON OF EXPERIMENTAL AND THEORETICAL VALUES

Experimental verification of the Gaussian model has followed a step-by-step procedure. Splice losses were measured between selected sets

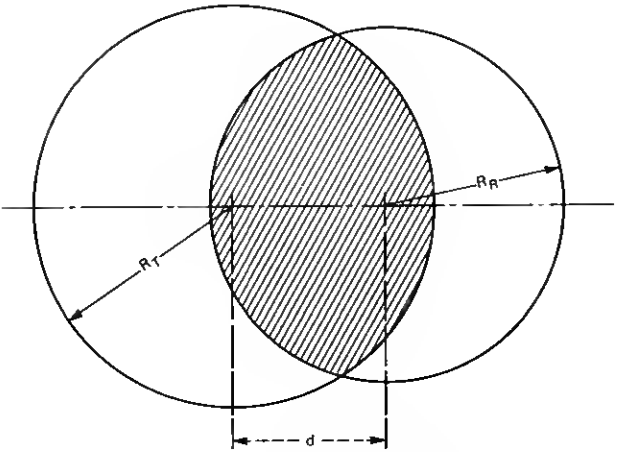

Fig. 2—Overlap regions for offset fiber cores.

of fibers which differed primarily in one intrinsic parameter. The results for Δ and radius mismatch were previously reported in Ref. 2, along with transverse offset results for both short and long receiving fibers. Results for α mismatch and combinations of intrinsic mismatch and transverse offset are given here.

All measurements were made using a pulsed, 0.82-μm, laser source with a pigtail which was loose-tube-spliced[6] to the transmitting fiber. The minimum length of the transmitting fiber was 550 m, except for one step index fiber (~250 m), to provide an approximate steady-state power distribution at the splice. The transmitting fiber was wound under tension to reproduce typical microbending losses found in some cables to simulate transmitting power distributions of interest. The receiving fiber was approximately 1 meter in length, though two tests were repeated using 10-m lengths to determine if any cladding modes were present. The results were essentially the same in either case.

IV. α MISMATCH

Splice loss due to α mismatch was measured for a few representative fiber pairs. The results are shown in Fig. 3 along with the general α mismatch curves generated by this model. The agreement between theory and measurement is good. For $\alpha_2 = 1.5$ and $\alpha_1 = 2.0$, a 25-percent mismatch in α, the splice loss is less than 0.2 dB. Sensitivity of splice loss to α mismatch is therefore substantially less than that for Δ or core radius mismatch.[2]

Fibers with combinations of α and Δ or α and radius mismatch were also spliced to observe the effects of combinations of factors. The results are given in Table I, where the first three columns indicate the percentage difference of each intrinsic parameter of the transmitting

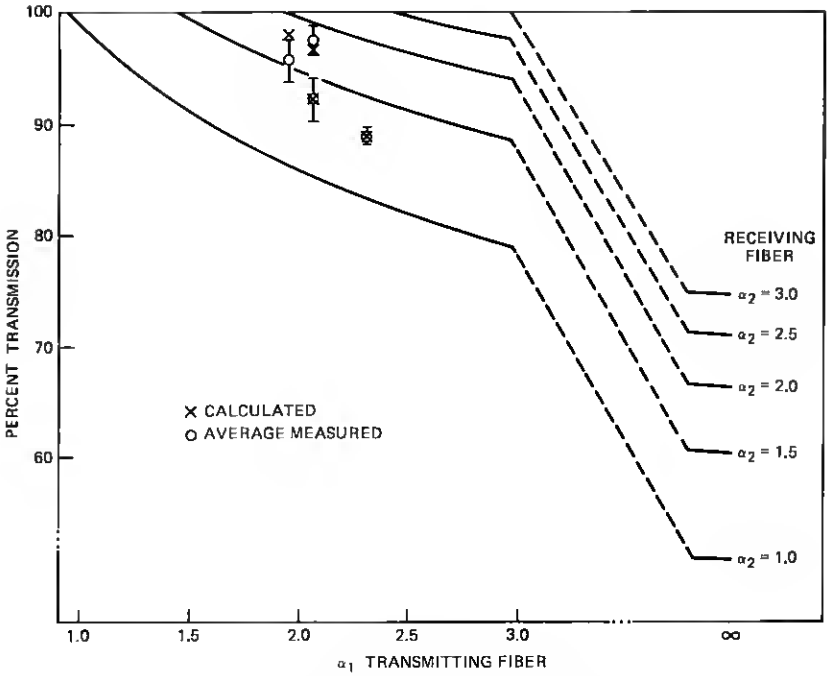

Fig. 3—Transmission vs α mismatch.

Table I—Calculated and measured splice losses between selected fiber pairs for α mismatch verification

Percentage Difference*			Predicted Loss (dB)	Measured Loss (dB)			Number of Readings
α	Δ	R		Low	Avg.	High	
+26.1	0	+6.3	0.374	0.258	0.357	0.458	6
+20.9	−3.5	0	0.105	0.053	0.110	0.156	7
−32.5	+37.6	0	0.558	0.564	0.614	0.667	5
+13.1	0	−1.1	0.074	0.101	0.189	0.276	7
+∞	−3.5	−14.8	0.864	0.442	0.585	0.674	8

* +26.1 indicates that the α of the transmitting fiber is 26.1 percent higher than the α of the receiving fiber.

fiber from those of the receiving fiber with the sign indicating the direction of the change (+ indicates a larger transmitting fiber parameter). The average measured loss is given, as well as the range and number of measurements. Each measurement involves disassembly of the splice, fracture of new ends on both fibers, and reassembly of the splice.

The range of loss measurements for some combinations of parameter mismatch is relatively large. Several factors contributed to this variation. (*i*) The detector used for early measurements degraded in its

repeatability properties and was replaced by a different detector for later measurements. These repeatability problems were primarily due to lack of precision in positioning the fiber relative to the detector. (*ii*) Failure of the lock-in amplifier to track frequency drift in the source was found to cause measurement variations of as much as ±0.1 dB. (*iii*) End quality and contamination, along with small variations in the positions of the fibers in the splices, also contribute to measurement variations. (*iv*) Fiber profile asymmetries may also contribute slightly to measurement variations.

An attempt was made to test the limits of applicability of the model by applying it to a splice between step-index ($\alpha = \infty$) and approximately parabolic-index fibers. The results, as shown in Table I, indicate that the model gives a fair estimate of the loss even in this extreme case when the Δ and radius mismatches are included in the calculation. The shortness of the step-index transmitting fiber in this case (250 m) may have caused an incomplete filling of the transmitting mode structure.

The results for general intrinsic parameter mismatch measurements are given in Table II. It can be seen that some measurements agree very well with the calculated values, while others vary on both the high and low sides. The average relative difference between theoretical and experimental values, $(1/n) \sum$ (calculated loss − measured loss), was 0.03 dB for all graded-index fiber data in Tables I and II. The average absolute difference, $(1/n) \sum$ |calculated loss − measured loss|, was 0.11 dB. It should be noted that inaccuracies in measuring α, Δ, and core radius as well as variations of α over the core probably account for some of the difference between theoretical and experimental values given here. The experimental data were accumulated over a three-month period using several different detectors. All the data are reported here. No systematic errors are apparent.

V. CORE ELLIPTICITY

Measurements of splice loss due to core ellipticity were made as a function of the angle between the major axes of the transmitting and receiving fibers (Fig. 4). This produced an approximately sinusoidal curve with zero loss at the 0° and 180° points and maximum loss at the 90° and 270° points. This maximum can be compared to the value calculated from the model.

The measurements were limited by a lack of suitable fibers with significant core ellipticity as well as by the low magnitude of the losses involved. Several fibers were selected which had core ellipticities of 4, 10, and 16.5 percent. The fibers with 4- and 10-percent ellipticity were too short to permit measurements with long fiber lengths after the splice. The maximum loss measured was less than 0.05 dB for the 4-percent fiber and less than 0.1 dB for the 10-percent fiber. The

Table II—Calculated and measured splice loss for general parameter mismatch verification

Percentage Difference			Predicted Loss	Measured Loss (dB)			Number of
α	Δ	R	(dB)	Low	Avg.	High	Readings
−5.1	−0.22	+0.4	0.001	0.059	0.090	0.156	6
+5.1	+0..22	−0.4	0.032	0.102	0.168	0.216	5
+33.3	−1.2	+7.8	0.495	0.468	0.497	0.537	5
+4.5	+7.6	+2.7	0.195	0.075	0.155	0.321	8
+24.6	+19.9	+0.8	0.579	0.275	0.296	0.310	5
−10.5	+50.0	+0.8	1.27	0.817	1.03	1.42	24
+21.0	+13.3	−1.9	0.340	0.171	0.216	0.260	5
+31.3	+13.3	−3.0	0.437	0.237	0.264	0.321	5
−14.6	+45.9	−1.9	0.996	0.703	0.876	1.06	12
−30.4	+36.8	+0.8	0.536	0.610	0.684	0.774	7

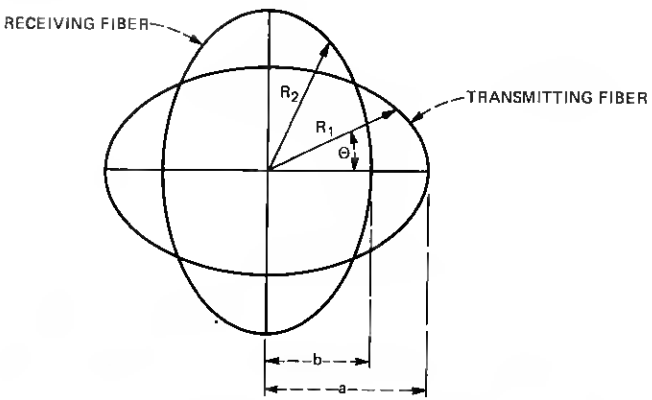

(a)

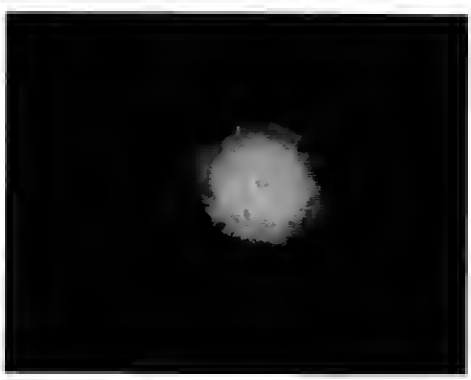

(b)

Fig. 4—Elliptical core fibers. (a) 90-degree core misalignment. (b) 16.5 percent ellipticity fiber core.

repeatability of the measurements is a few hundredths of a decibel. This prevented an accurate determination of the effect of the ellipticity. These losses were approximately the same as those predicted by the Gaussian model (0.025 dB for 4 percent and 0.08 dB for 10 percent) (Fig. 5) and significantly less than those predicted by the uniform power model (0.12 dB for 4 percent and 0.325 dB for 10 percent). Figure 4b shows the core cross section of the 16.5-percent fiber. Although not a perfect ellipse, this was the only fiber available with sufficient ellipticity to give a splice loss large enough to be accurately measured.

The 16.5-percent ellipticity fiber was an extremely high loss fiber, ~50 dB/km for long sections of fiber. The near-field patterns for a 100-m length and an 800-m length were essentially the same, and it appeared that the high-loss characteristics of the fiber produced full mode coupling in the 100-m length. For this reason, it was felt that the

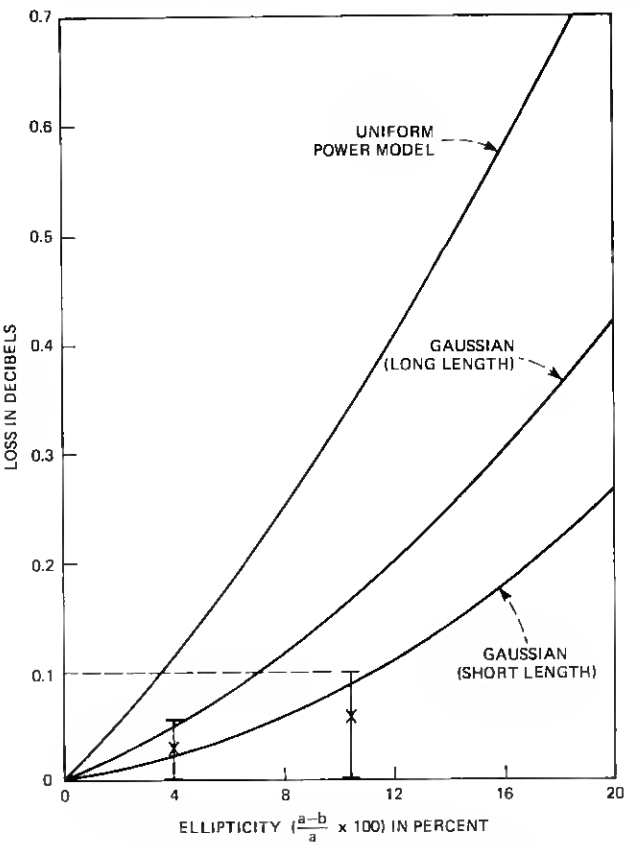

Fig. 5—Maximum splice loss due to core ellipticity.

100-m length was sufficient to satisfy the assumption (in both Gaussian and uniform power models) of a steady-state power distribution entering the splice.

Figure 6 shows the splice loss for this fiber with a 1-m length after the splice as a function of the angle between the semi-major axes of the ellipses. The general shape of a curve through the data points and the average maximum loss of 0.13 dB are in good agreement with the expected shape and the value calculated from the model of 0.19 dB. The discrepancies may be partly attributable to the deviation from pure ellipticity of the core cross section as shown in Fig. 4b and to the shortness of the transmitting fiber. The difference between the average maximum measured loss and the loss calculated with the Gaussian model was only 0.06 dB. This was approximately the same as the noise and repeatability properties of the measurement system.

Figure 7 shows the results when a 100-m length of receiving fiber is used. Again the general shape of the curve agrees with that expected, although more noise is apparent in the data. The average maximum splice loss was 0.18 dB which is in fair agreement with the calculated value of 0.31 dB. Measurements with longer lengths of receiving fiber were attempted, but the results were inconclusive because of the high attenuation and reduced signal-to-noise ratio.

VI. INTRINSIC MISMATCH PLUS TRANSVERSE OFFSET

Experimental and theoretical values for splice loss vs transverse offset with intrinsic parameter mismatch are shown in Fig. 8. The fibers used in this part correspond to line 9 in Table II. The experimental points represent the average of four readings, two left of center and two right of center, as the receiving fiber was traversed across the transmitting fiber. The agreement is very good.

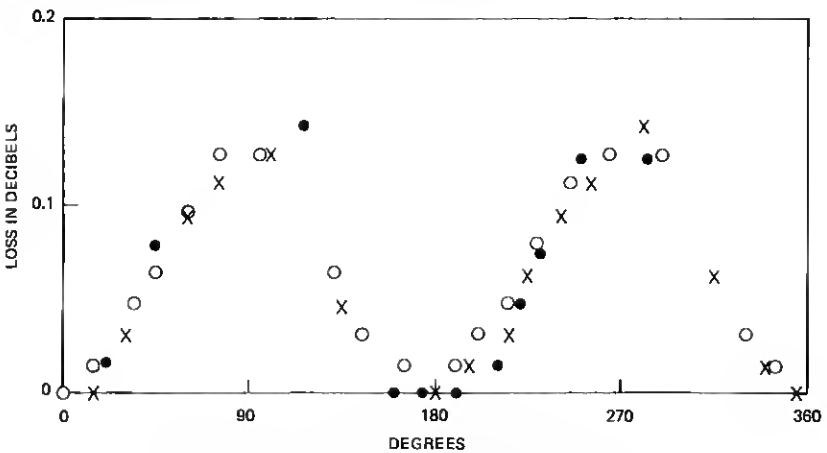

Fig. 6—Core ellipticity splice loss, short length.

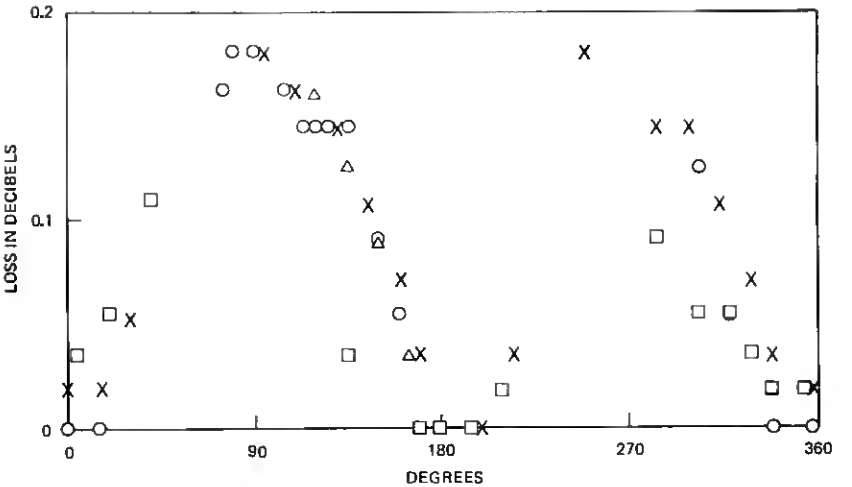

Fig. 7—Core ellipticity splice loss, long length.

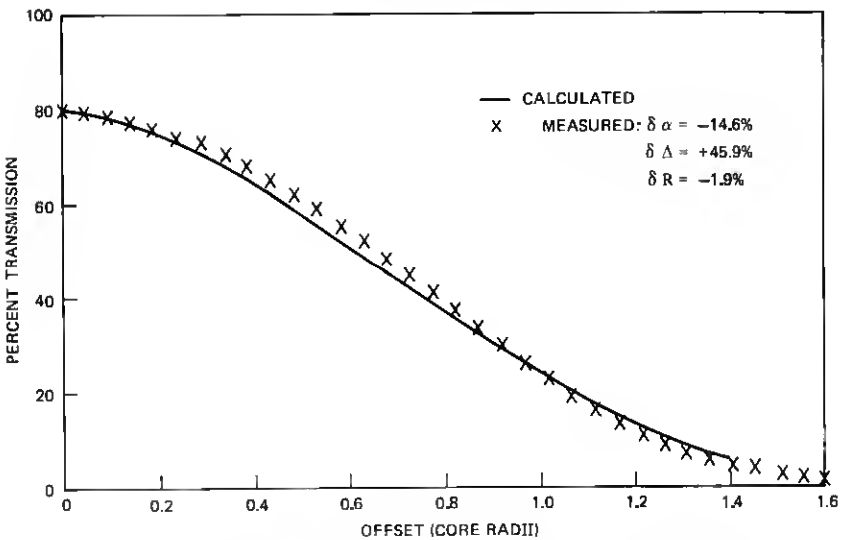

Fig. 8—Intrinsic parameter mismatch and transverse offset.

The model can also be used to generate parametric families of curves such as Fig. 9 and Fig. 10, showing the importance of the different intrinsic parameters when combined with an extrinsic parameter. Δ mismatch and transverse offset are shown in Fig. 9 and radius mismatch and transverse offset in Fig. 10, since they are the chief intrinsic and extrinsic factors contributing to splice loss at this time. In particular, Fig. 9 emphasizes that, if the receiving fiber NA is greater than the transmitting fiber NA, the sensitivity to transverse offset is significantly reduced, especially for small offsets. Sensitivity to transverse

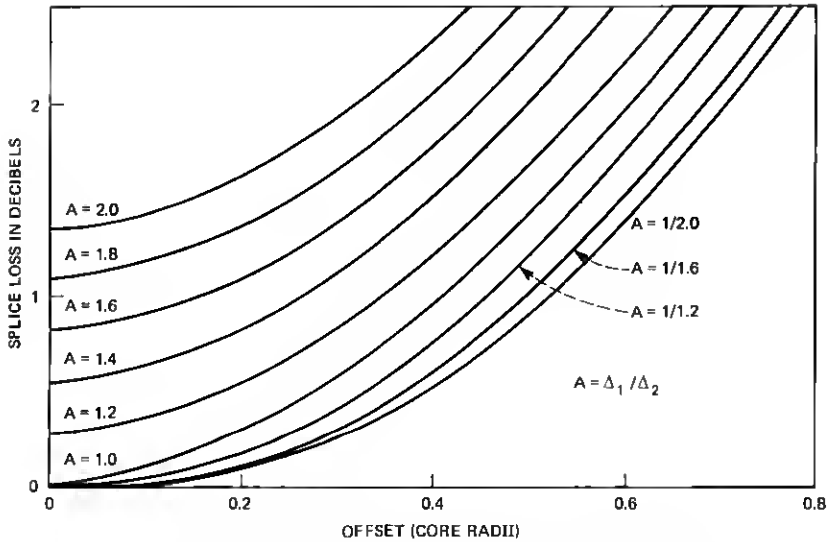

Fig. 9—Splice loss due to Δ mismatch and transverse offset.

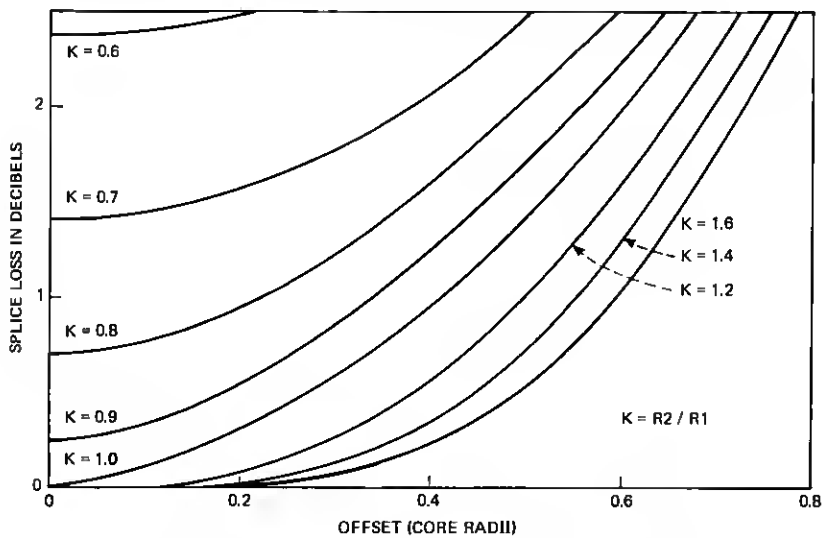

Fig. 10—Splice loss due to radius mismatch and transverse offset.

offset is slightly reduced for a receiving fiber NA less than the transmitting fiber NA, in fact, the maximum sensitivity to transverse offset occurs for identical fibers.

VII. CONCLUSION

It has been demonstrated that the Gaussian point transmission model gives good estimates of splice loss due to intrinsic parameter

mismatch and transverse offset. The effects of combinations of these factors on splice loss has been characterized and shown to be significant. Effects due to α and ϵ mismatch are smaller for a given percentage mismatch than for Δ or core radius mismatches.

VIII. ACKNOWLEDGMENT

The author is grateful to C. M. Miller for his advice and for calculating the long length and the uniform power model losses and to D. N. Ridgway for his assistance with the experimental measurements. Thanks are also due to M. J. Saunders for providing the intrinsic parameters of the fibers used in this experiment, to F. T. Stone for providing both the 16.5-percent elliptical core fiber and the photograph of its core, and to M. I. Schwartz for help in organizing this paper.

APPENDIX

This section provides more detail on the application of this theory to various general classes of fiber splices. The integrals in eq. (7) cannot be performed exactly, except in a few special cases. Numerical evaluation is usually required, but considerable simplification can sometimes result from careful consideration of the particular splice parameters. The case of intrinsic parameter mismatch with no ellipticity and no transverse offset is examined first.

A1. Splices without transverse offset

Zero offset splices can be broken down into three classes for the particular family of radially symmetric profiles assumed here.

Class I contains splices with all transmitting parameters greater than or less than all corresponding receiving parameters. Class Ia is illustrated in Fig. 11a.

$$\text{Class Ia:} \begin{cases} \alpha_1 \geq \alpha_2 \\ \Delta_1 \geq \Delta_2 \\ R_1 \geq R_2 \end{cases} \qquad \text{Class Ib:} \begin{cases} \alpha_1 \leq \alpha_2 \\ \Delta_1 \leq \Delta_2 \\ R_1 \leq R_2 \end{cases}$$

For Ia

$$P_2 = \int t(r)(1 - k^{\alpha_1} r^{\alpha_1})^2 r dr. \tag{8}$$

For Ib the transmission equals unity.

Class II splices have one intersection of the core profile. Class IIa is shown in Fig. 11b.

$$\text{Class IIa:} \begin{cases} \Delta_1 > \Delta_2 \\ R_1 < R_2 \end{cases} \qquad \text{Class IIb:} \begin{cases} \Delta_1 < \Delta_2 \\ R_1 > R_2 \end{cases}$$

In both these cases, the transmission is unity wbere NA_2 exceeds NA_1 and a function of r over the remainder of the profile. The crossover point, r', is determined by equating tbe NAs and solving the resulting nonlinear equation numerically:

$$\Delta_1(1 - k^{\alpha_1} r^{\alpha_1}) = \Delta_2(1 - r^{\alpha_2}). \tag{9}$$

Then

$$P_2 = \begin{cases} \displaystyle\int_0^{r'} t(r)(1 - k^{\alpha_1} r^{\alpha_1})^2 r\,dr + \int_{r'}^{1} (1 - k^{\alpha_1} r^{\alpha_1})^2 r\,dr & \text{IIa} \\ \displaystyle\int_0^{r'} (1 - k^{\alpha_1} r^{\alpha_1})^2 r\,dr + \int_{r'}^{1/k} t(r)(1 - k^{\alpha_1} r^{\alpha_1})^2 r\,dr & \text{IIb} \end{cases} \tag{10}$$

Class III contains all remaining possibilities. Class IIIa is shown in Fig. 11c.

$$\text{Class IIIa: } \begin{cases} \Delta_1 \geq \Delta_2 \\ \alpha_1 < \alpha_2 \\ R_1 \geq R_2 \end{cases} \qquad \text{Class IIIb: } \begin{cases} \Delta_1 \leq \Delta_2 \\ \alpha_1 > \alpha_2 . \\ R_1 \leq R_2 \end{cases}$$

Class III mismatches may or may not have the crossovers shown in Fig. 11c. Those that do not cross over correspond to Fig. 11a; however, it is necessary to solve eq. (9) to determine whether a crossover occurs. If no r' exists, the loss can be calculated using the appropriate formula for Class I. If an r' exists, the second crossover point r'' must also be found to determine the appropriate areas of integration. Again, the transmission is unity where NA_2 is greater than NA_1 and is a function of r over the rest of the profile. Then

$$P_2 = \begin{cases} \displaystyle\int_0^{r'} t(r)(1 - k^{\alpha_1} r^{\alpha_1})^2 r\,dr + \int_{r'}^{r''} (1 - k^{\alpha_1} r^{\alpha_1})^2 r\,dr \\ \qquad\qquad + \displaystyle\int_{r'}^{1} t(r)(1 - k^{\alpha_1} r^{\alpha_1})^2 r\,dr & \text{IIIa} \\ \displaystyle\int_0^{r'} (1 - k^{\alpha_1} r^{\alpha_1})^2 r\,dr + \int_{r'}^{r''} t(r)(1 - k^{\alpha_1} r^{\alpha_1})^2 r\,dr \\ \qquad\qquad + \displaystyle\int_{r''}^{1/k} (1 - k^{\alpha_1} r^{\alpha_1})^2 r\,dr & \text{IIIb} \end{cases} \tag{11}$$

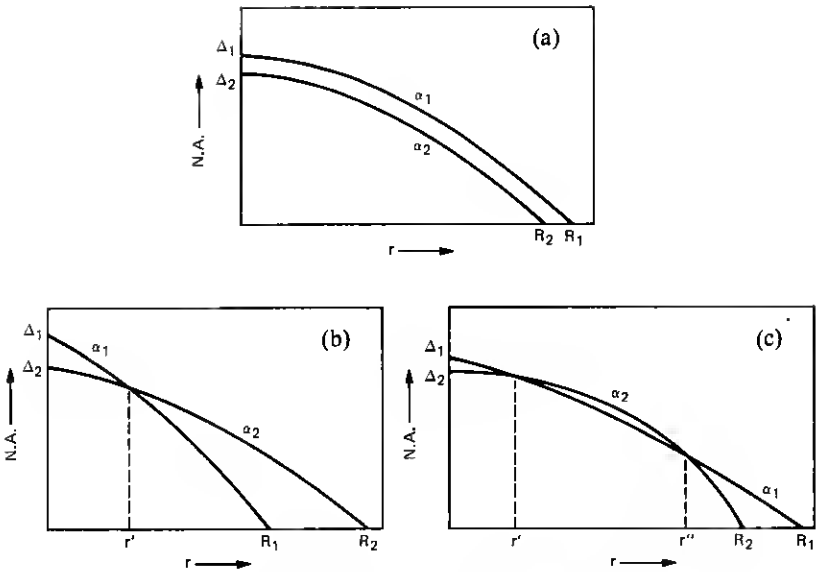

Fig. 11—Intrinsic mismatch profiles. (a) Class Ia. (b) Class IIa. (c) Class IIIa.

Two special cases also occur when $\Delta_1 = \Delta_2$ or $\alpha_1 = \alpha_2$.

If $\Delta_1 = \Delta_2$ (Class III):

$$r' = k^{\left(\frac{\alpha_1}{\alpha_2 - \alpha_1}\right)}. \tag{12}$$

In this special case, r' exists only if $R_1 > R_2$ and $\alpha_1 < \alpha_2$ or $R_1 < R_2$ and $\alpha_1 > \alpha_2$. Otherwise, the only crossover is at $r = 0$.

If $\alpha_1 = \alpha_2 = \alpha$ (Class II):

$$r' = \left(\frac{\Delta_2 - \Delta_1}{\Delta_2 - k^\alpha \Delta_1}\right)^{1/\alpha}. \tag{13}$$

If $\alpha_1 = \alpha_2$ in Class I or III, there is no crossover.

A2. Splices with transverse offset

The addition of transverse offset greatly complicates the problem. The four cases of Ref. 4 must be included and the integrals evaluated over the areas of overlap. The power transmitted at any point is the product of the point transmission function, $t(r)$, and the power available to be transmitted at that point.

$$p(r) = t(r)(1 - k^{\alpha_1} r^{\alpha_1})^2. \tag{14}$$

However, since the cores are not centered, one of the NA functions must be transformed to the center of the other core. The integral can

then be performed numerically setting $t(r)$ equal to unity at any point at which NA_2 is greater than NA_1. In the cases in which the two core boundaries do not intersect, Cases I and III of Ref. 4, one obtains a double integral referenced to the center of the smaller core. This is illustrated in Fig. 12a. The definition of d is the normalized separation of the fiber core centers.

Case I: $R_1 < R_2$, $d < 1 - 1/k$.

$$d = \frac{\text{Transverse Offset}}{R_2} \quad (R_2 = \text{receiving fiber core radius}) \tag{15}$$

$$P_2 = 2\int_0^{\pi}\int_0^{1/k} t_1(r)(1 - k^{\alpha_1}r^{\alpha_1})^2 r\,dr\,d\theta \tag{16}$$

$$t_1(r) = \begin{cases} 1 + Q_1 p_0 - p_0^{Q_1} & Q_1 < 1 \\ 1 & Q_1 \geq 1 \end{cases}. \tag{17}$$

$$Q_1 = \frac{\Delta_2[1 - (r^2 + d^2 - 2rd\cos\theta)^{\alpha_2/2}]}{\Delta_1(1 - k^{\alpha_1}r^{\alpha_1})}. \tag{18}$$

Case III: $R_1 > R_2$, $d < 1/k - 1$.

$$P_2 = 2\int_0^{\pi}\int_0^{1} t_2(r)[1 - k^{\alpha_1}(r^2 + d^2 - 2rd\cos\theta)^{\alpha_1/2}]^2 r\,dr\,d\theta \tag{19}$$

$$t_2(r) = \begin{cases} 1 + Q_2 p_0 - p_0^{Q_2} & Q_2 < 1 \\ 1 & Q_2 \geq 1 \end{cases}. \tag{20}$$

$$Q_2 = \frac{\Delta_2(1 - r^{\alpha_2})}{\Delta_1[1 - k^{\alpha_1}(r^2 + d^2 - 2rd\cos\theta)^{\alpha_1/2}]}. \tag{21}$$

Cases II and IV of Ref. 4 present two different possible conditions of overlap requiring different approaches to the numerical integration. These are illustrated in Figs. 12b and 12c. The area of overlap is divided into regions which permit the use of the functions $t_1(r)$ and $t_2(r)$ defined above. The two separate conditions are distinguished by the following criteria:

Case II: $R_2 > R_1$ and $d > 1 - 1/k$ (interchange R_2 and R_1 in Fig. 12).

Condition 1: $1 - \frac{1}{k^2} - d^2 \leq 0$: Fig. 12b

Condition 2: $1 - \frac{1}{k^2} - d^2 > 0$: Fig. 12c.

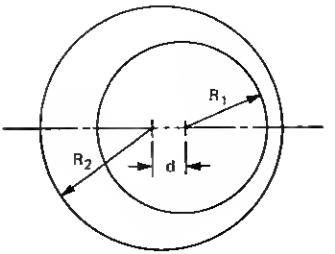

(a)

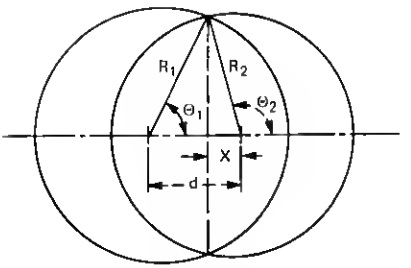

(b)

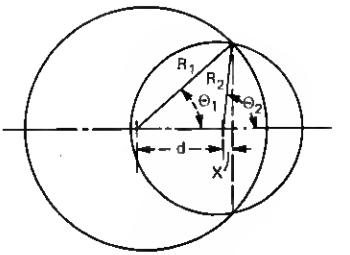

(c)

Fig. 12—Parameter mismatch and transverse offset. (a) Cases I and III offset. (b) Condition I $\theta_2 > \pi/2$. (c) Condition II $\theta_2 < \pi/2$.

Case IV: $R_2 < R_1$ and $d > 1/k - 1$.

Condition 1: $\frac{1}{k^2} - 1 - d^2 \leq 0$: Fig. 12b

Condition 2: $\frac{1}{k^2} - 1 - d^2 > 0$: Fig. 12c.

In practice, the two different conditions in Cases II and IV are distinguished by the sign of $\cos \theta_2$.

Case II:

$$\cos \theta_1 = \frac{1 + d^2 - 1/k^2}{2d} \tag{22}$$

$$\cos \theta_2 = \frac{1 - d^2 - 1/k^2}{2d}. \tag{23}$$

Condition I: $\cos \theta_2 < 0$ (Fig. 12b).

$$P_2 = \int_0^{\theta_1} \int_{\frac{d-x}{\cos\theta}}^{1} t_2(r)[1 - k^{\alpha_1}(r^2 + d^2 - 2rd\cos\theta)^{\alpha_1/2}]^2 r dr d\theta$$

$$+ \int_{\pi-\theta_2}^{\pi} \int_{\frac{x}{\cos\theta}}^{1/k} t_1(r)(1 - k^{\alpha_1} r^{\alpha_1})^2 r dr d\theta, \tag{24}$$

where

$$x = \frac{d^2 + 1/k^2 - 1}{2d}. \tag{25}$$

Condition II: $\cos \theta_2 > 0$ (Fig. 12c).

$$P_2 = \int_0^{\theta_1} \int_{\frac{d+x}{\cos\theta}}^{1} t_2(r)[1 - k^{\alpha_1}(r^2 + d^2 - 2rd\cos\theta)^{\alpha_1/2}]^2 r dr d\theta$$

$$+ \int_0^{\theta_2} \int_0^{\frac{x}{\cos\theta}} t_1(r)(1 - k^{\alpha_1} r^{\alpha_1})^2 r dr d\theta,$$

$$+ \int_{\theta_2}^{\pi} \int_0^{1/k} t_1(r)(1 - k^{\alpha_1} r^{\alpha_1})^2 r dr d\theta \tag{26}$$

where

$$x = \frac{1 - d^2 - 1/k^2}{2d}. \tag{27}$$

Case IV:

$$\cos\theta_1 = \frac{1/k^2 + d^2 - 1}{2d} \tag{28}$$

$$\cos\theta_2 = \frac{1/k^2 - d^2 - 1}{2d}. \tag{29}$$

Condition I: $\cos \theta_2 < 0$ (Fig. 12b).

$$P_2 = \int_0^{\theta_1} \int_{\frac{d-x}{\cos\theta}}^{1/k} t_1(r)(1 - k^{\alpha_1} r^{\alpha_1})^2 r dr d\theta$$

$$+ \int_{\pi-\theta_2}^{\pi} \int_{\frac{x}{\cos\theta}}^{1} t(r)[1 - k^{\alpha_1}(r^2 + d^2 - 2rd\cos\theta)^{\alpha_1/2}]^2 r dr d\theta, \tag{30}$$

where

$$x = \frac{1 + d^2 - 1/k^2}{2d}. \tag{31}$$

Condition II: $\cos\theta_2 > 0$ (Fig. 12c).

$$P_2 = \int_0^{\theta_1} \int_{\frac{d+x}{\cos\theta}}^{1/k} t_1(r)(1 - k^{\alpha_1} r^{\alpha_1})^2 r dr d\theta$$

$$+ \int_0^{\theta_2} \int_0^{\frac{x}{\cos\theta}} t_2(r)[1 - k^{\alpha_1}(r^2 + d^2 - 2rd\cos\theta)^{\alpha_1/2}]^2 r dr d\theta$$

$$+ \int_{\theta_2}^{\pi} \int_0^{1} t_2(r)[1 - k^{\alpha_1}(r^2 + d^2 - 2rd\cos\theta)^{\alpha_1/2}]^2 r dr d\theta, \qquad (32)$$

where

$$x = \frac{1/k^2 - d^2 - 1}{2d}. \qquad (33)$$

Application of the Gaussian model to the case of elliptical mismatch is restricted to identical fibers with no transverse offset. The splice loss in this case will vary from zero, when the axes of the elliptical cores are perfectly aligned, to some maximum, when they are at right angles to each other. For identical elliptical fibers, the Gaussian model was used to calculate the maximum loss.

Figure 4a illustrates the geometry of the maximum loss case. For identical fibers, $\alpha_1 = \alpha_2 = \alpha$, $\Delta_1 = \Delta_2$ and $a_1 = a_2$ and $b_1 = b_2$ where a and b are the semimajor and semiminor axes of the elliptical core and the subscripts 1 and 2 refer to the transmitting and receiving fibers, respectively. The symmetry of the system shown was used to reduce the calculation of the fraction of the power transmitted through the splice to one quadrant.

At any angle θ,

$$k(\theta) \equiv \frac{R_2}{R_1} = \sqrt{\frac{a^2\sin^2\theta + b^2\cos^2\theta}{a^2\cos^2\theta + b^2\sin^2\theta}}. \qquad (34)$$

Then Q, the ratio of the numerical apertures squared at any point in the splice, is

$$Q(r, \theta) = \frac{1 - r^{\alpha}}{1 - k^{\alpha} r^{\alpha}} \qquad (35)$$

for $0 \le \theta \le \Pi/4$, $r \le R_2$ and for $\Pi/4 \le \theta \le \Pi/2$, $r \le R_1$. The total

transmission ratio with R_2 normalized to unity is

$$T = \frac{P_2}{P_1}$$

$$= \frac{\int_0^{\pi/4} \int_0^1 t(r, \theta)(1 - k^\alpha r^\alpha)^2 r dr d\theta + \int_{\pi/4}^{\pi/2} \int_0^{1/k} (1 - k^\alpha r^\alpha)^2 r dr d\theta}{\int_0^{\pi/2} \int_0^{1/k} (1 - k^\alpha r^\alpha)^2 r dr d\theta}. \quad (36)$$

The point transmission from 45° to 90° in the first quadrant is unity since the receiving numerical aperture is larger than the transmitting numerical aperture in this region. Solution of the integrals in eq. (36) by numerical methods gives the results shown in Fig. 5 for the maximum loss due to core ellipticity. The long length loss was found by correcting for the additional loss in a long fiber due to mode redistribution.[2]

The uniform power model loss was found using eq. (36) with $t(r, \theta)$ set equal to Q, the ratio of the squares of the numerical apertures, using $1 - k^\alpha r^\alpha$ as the near-field power function. The difference between the Gaussian model and the uniform power model is appreciably greater for elliptical mismatch than for the other intrinsic mismatches due to the greater difference between the two models near the core-cladding boundary.

REFERENCES

1. D. Gloge and E. A. J. Marcatili, "Multimode Theory of Graded-Core Fibers," B.S.T.J., *52*, No. 9 (November 1973), pp. 1563–1578.
2. C. M. Miller and S. C. Mettler, "A Loss Model for Parabolic-Profile Fiber Splices," B.S.T.J., *57*, No. 9 (November 1978), pp. 3167–3180.
3. Haruhiko Tsuchiya et al., "Double Eccentric Connectors for Optical Fibers," Appl. Opt., *16*, No. 5 (May 1977), pp. 1323–1331.
4. C. M. Miller, "Transmission vs. Transverse Offset for Parabolic-Profile Fiber Splices witb Unequal Core Diameters," B.S.T.J., *55*, No. 7 (September 1976), pp. 917–927.
5. C. M. Miller, "Effects of Fiber Manufacturing Variations on Graded Index Fiber Splices," Proc. 4th European Conference on Optical Communication, Genoa, Italy, September 12–15, 1978.
6. C. M. Miller, "Loose Tube Splices for Optical Fibers," B.S.T.J., *54*, No. 7 (September 1975), pp. 1215–1225.